



## BIROn - Birkbeck Institutional Research Online

Crawford, Ian and Craig, N. and Welsh, B.Y. (1997) The velocity structure of the local interstellar medium probed by ultra-high-resolution spectroscopy. *Astronomy & Astrophysics* 317 (3), pp. 889-897. ISSN 0004-6361.

Downloaded from: <https://eprints.bbk.ac.uk/id/eprint/28542/>

*Usage Guidelines:*

Please refer to usage guidelines at <https://eprints.bbk.ac.uk/policies.html> or alternatively contact [lib-eprints@bbk.ac.uk](mailto:lib-eprints@bbk.ac.uk).

# The velocity structure of the local interstellar medium probed by ultra-high-resolution spectroscopy

I.A. Crawford<sup>1</sup>, N. Craig<sup>2</sup>, and B.Y. Welsh<sup>2</sup>

<sup>1</sup> Department of Physics and Astronomy, University College London, Gower Street, London, WC1E 6BT, UK

<sup>2</sup> Space Sciences Laboratory, University of California, Berkeley, CA 94720, USA

Received 25 March 1996 / Accepted 2 May 1996

**Abstract.** We present ultra-high-resolution ( $0.35 \text{ km s}^{-1}$  FWHM) observations of the interstellar Ca K line towards eight nearby stars (six of which are closer than 30 pc). The spectral resolution is sufficient to resolve the line profiles fully, thereby enabling us to detect hitherto unresolved velocity components, and to obtain accurate measurements of the velocity dispersions ( $b$ -values). Absorption components due to the Local Interstellar Cloud (LIC) and/or the closely associated ‘G Cloud’ are identified towards all but one star ( $\gamma$  Oph), but only in one case (51 Oph) are *both* clouds reliably detected towards the same star. Most of these nearby clouds have velocity dispersions ( $b \approx 2 \text{ km s}^{-1}$ ) which suggest physical conditions similar to those inferred for the LIC ( $T_k \approx 7000 \text{ K}$ ,  $v_t \approx 1 \text{ km s}^{-1}$ ), although at least three lines of sight (towards  $\gamma$  Aqr,  $\beta$  Cen and  $\rho$  Cen) also sample cooler and/or less turbulent material. The spectrum of the nearby Vega-excess star 51 Oph is of particular interest, owing to evidence that several of the absorption components arise in the circumstellar environment.

**Key words:** ISM: clouds – ISM: kinematics and dynamics – ISM: structure – ISM: atoms

## 1. Introduction

There is now considerable evidence that the Sun lies within a warm ( $T \sim 7000 \text{ K}$ ) low-density ( $n_H \sim 0.1 \text{ cm}^{-3}$ ) interstellar cloud, and that this Local Interstellar Cloud (LIC) is itself located within the hot ( $T \sim 10^6 \text{ K}$ ) and empty ( $n_H \sim 0.005 \text{ cm}^{-3}$ ) Local Bubble in the interstellar medium (see Cox & Reynolds 1987 and Frisch 1995 for reviews). Our knowledge of the Local Bubble has improved greatly in recent years, as a result of observations performed at optical, ultraviolet and X-ray wavelengths. Recent results from the ROSAT wide-field camera (Diamond et al. 1995), EUVE (Vennes et al. 1994), and

ground-based optical spectroscopy (Welsh et al. 1994) all confirm the distinct lack of neutral gas within  $\sim 50 \text{ pc}$  of the Sun. The evidence that this volume is filled with a high-temperature plasma comes primarily from observations of the soft X-ray background (McCammon et al. 1983, McCammon & Sanders 1990), although it has been pointed out by Breitschwerdt & Schmutzler (1994) and Jelinsky, Vallerga & Edelstein (1995) that if the gas is out of ionisation equilibrium the temperature might be considerably lower than generally assumed.

Our knowledge of the low-density clouds within the Local Bubble has also improved, largely owing to the ability of modern high-resolution spectrographs to detect the weak absorption lines (equivalent widths of a few mÅ) which these clouds produce in the spectra of nearby stars. This work has revealed that, within a few tens of parsecs of the Sun, the Local Bubble contains several small clouds with characteristics apparently similar to those of the LIC (Lallement et al. 1986, 1994; Bertin et al. 1993). Using ground-based and HST-GHRS observations, Lallement et al. (1995) have deduced that the LIC is moving past the Solar System with a heliocentric velocity of  $26 \pm 1 \text{ km s}^{-1}$  towards  $l = (186 \pm 3)^\circ$ ,  $b = (-16 \pm 3)^\circ$ . In addition, they (see also Lallement & Bertin 1992) have drawn attention to another nearby cloud, characterised by a slightly different velocity vector ( $29 \text{ km s}^{-1}$  towards  $l = 184.5^\circ$ ,  $b = -20.5^\circ$ ), which they designate as the ‘G Cloud.’ However, it is still unclear whether the G cloud is separate from the LIC, or is contiguous with it. As reviewed by Frisch (1995), these velocity vectors are consistent with a general outflow from the Scorpio-Centaurus OB Association ( $l \approx 320^\circ$ ,  $b \approx +10^\circ$ ) which appears to dominate the large scale kinematics of the local interstellar medium (LISM).

The temperature of the LIC in the immediate vicinity of the Solar System has been determined from observations of back-scattered solar Ly- $\alpha$  ( $8000 \pm 1000 \text{ K}$ ; Bertaux et al. 1985) and He I  $\lambda 584$  ( $7000 \pm 2000 \text{ K}$ ; Chassefiere, Dalaudier & Bertaux 1988). An essentially identical temperature ( $6700 \pm 1500 \text{ K}$ ) has been measured directly for interstellar He atoms in the outer Solar System from the *Ulysses* spacecraft (Witte et al. 1993). Evidence that this temperature is common to the LIC, rather than just that part of it impinging on the Solar System, is provided by

**Table 1.** List of the nearby stars observed for the interstellar Ca K line using the UHRF.  $v_{LIC}$  and  $v_G$  are the projected heliocentric velocities of the Local Interstellar and G clouds towards each of these stars (Lallement et al. 1995). The last column gives the total number of counts (electrons) obtained in the local continuum for each 24- $\mu$ m spectral element adjacent to the interstellar lines (generally this is formed by the core of the stellar photospheric Ca K line.)

Star	$V$	Sp.	$l$	$b$	Dist (pc) (ref)	$v_{LIC}$ (km s $^{-1}$ )	$v_G$ (km s $^{-1}$ )	Exposures ( $n \times$ secs)	Counts ( $e^-$ )
$\gamma$ Aqr	3.8	A0 V	62.2	-45.8	23 (1)	$-4.6 \pm 1.3$	$-2.8 \pm 1.5$	$1 \times 1200$	$8.8 \times 10^3$
$\beta$ Cen	0.6	B1 III	311.8	+1.3	81 (2)	$-14.8 \pm 1.2$	$-16.7 \pm 1.3$	$2 \times 1200$	$3.6 \times 10^5$
$\iota$ Cen	2.8	A2 V	309.4	+25.8	17 (1)	$-15.5 \pm 1.2$	$-18.4 \pm 1.3$	$4 \times 1200$	$4.6 \times 10^4$
$\rho$ Cen	4.0	B3 V	296.8	+10.0	83 (3)	$-10.0 \pm 1.3$	$-11.9 \pm 1.4$	$2 \times 1200$	$1.6 \times 10^4$
$\epsilon$ Gru	3.5	A3 V	338.3	-56.5	23 (1)	$-6.2 \pm 1.3$	$-5.0 \pm 1.5$	$5 \times 1200$	$2.2 \times 10^4$
$\alpha$ Hyi	2.9	F0 III	289.5	-53.8	25 (1)	$+2.3 \pm 1.3$	$+4.0 \pm 1.5$	$4 \times 1200$	$6.8 \times 10^3$
$\gamma$ Oph	3.8	A0 V	28.0	+15.4	29 (1)	$-24.2 \pm 1.0$	$-26.7 \pm 1.1$	$5 \times 1200$	$8.1 \times 10^3$
51 Oph	4.8	B9.5 V	2.5	+5.3	25 (1)	$-25.5 \pm 1.0$	$-28.0 \pm 1.0$	$6 \times 1200$	$1.5 \times 10^4$

References: (1) van Altena et al. (1991); (2) Lesh (1972); (3) de Geus et al. (1989).

Linsky et al. (1993, 1995), who obtained a value of  $7000 \pm 500$  K from HST observations of interstellar D I, Fe II and Mg II towards Procyon ( $\alpha$  CMi;  $D = 3.5$  pc) and Capella ( $\alpha$  Aur;  $D = 12.5$  pc). More recently, Linsky & Wood (1995) have obtained a similar, although somewhat lower, temperature of  $5400 \pm 500$  K from interstellar lines towards  $\alpha$  Cen A ( $D=1.3$  pc). These authors have also measured the rms turbulent velocities,  $v_t$ , for the LIC towards these stars, and found it to be of the order of  $1 \text{ km s}^{-1}$  (specifically,  $1.13 \pm 0.28 \text{ km s}^{-1}$  for Capella and Procyon, and  $0.85 \pm 0.18 \text{ km s}^{-1}$  for  $\alpha$  Cen; Linsky et al. 1995, Linsky & Wood 1995). [Note that in their papers, Linsky et al. characterise the turbulence by the parameter  $\xi$ , where  $\xi = \sqrt{2} \times v_t$  as used here; cf. Equation 1 below.]

Here we report observations of the interstellar Ca K line towards eight nearby stars obtained with the Ultra-High-Resolution Facility (UHRF) at the Anglo-Australian Telescope. The UHRF is currently the world's highest resolution astronomical spectrograph, and has been described in detail by Diego et al. (1995). The maximum resolving power is  $R \equiv \lambda/\Delta\lambda \approx 10^6$  ( $0.3 \text{ km s}^{-1}$  FWHM), which is more than an order of magnitude higher than most other instruments. As discussed by Crawford & Dunkin (1995), use of this very high resolving power has two main advantages for the study of the LISM: (1) it makes possible the resolution of closely-spaced velocity components, and therefore separation of the LIC from other nearby clouds; and (2) it enables us to measure reliable intrinsic line widths ( $b$ -values), thereby providing information on the temperature and turbulence within the clouds.

## 2. Observations

The observations were obtained in July 1995, and details of individual exposures are given in Table 1. The detector was a Tektronix CCD ( $1024 \times 1024$  24- $\mu$ m pixels). The spectrograph was used in conjunction with an image-slicer (Diego 1993), and the output was binned by a factor of eight perpendicular to the dispersion direction in order to reduce the readout noise associated with the broad spectrum which results. At the wavelength of the Ca K line ( $3933.663 \text{ \AA}$ ) the dispersion was  $0.086 \text{ \AA mm}^{-1}$ , giving a spectral coverage of  $2.1 \text{ \AA}$ . The resolution, measured with the aid of a stabilized He-Ne laser, was  $0.350 \pm 0.004 \text{ km s}^{-1}$  (FWHM), corresponding to a resolving power of  $R = 860,000$ .

The CCD images were divided by a flatfield, and the spectra extracted using the FIGARO data-reduction package (Shortridge 1988). Background light was measured from the inter-order region and subtracted. Wavelength calibration was performed using a Th-Ar comparison lamp. Second-order polynomial fits to between 5 and 7 comparison lines yielded typical rms residuals of  $5 \times 10^{-4} \text{ \AA}$  ( $0.04 \text{ km s}^{-1}$ ); in no case were the rms residuals greater than  $8 \times 10^{-4} \text{ \AA}$  ( $0.06 \text{ km s}^{-1}$ ). Once wavelength calibrated the spectra were converted to the heliocentric velocity frame, and multiple exposures (Table 1) were co-added. Most of these stars exhibit strong photospheric Ca K lines, the cores of which act as the local continua for the interstellar lines. These were fitted by low-order polynomials and divided out, to give the normalised spectra shown in Fig. 1.

## 3. Results

The heliocentric velocities, velocity dispersions ( $b$ -values), and Ca II column densities were obtained for each velocity com-

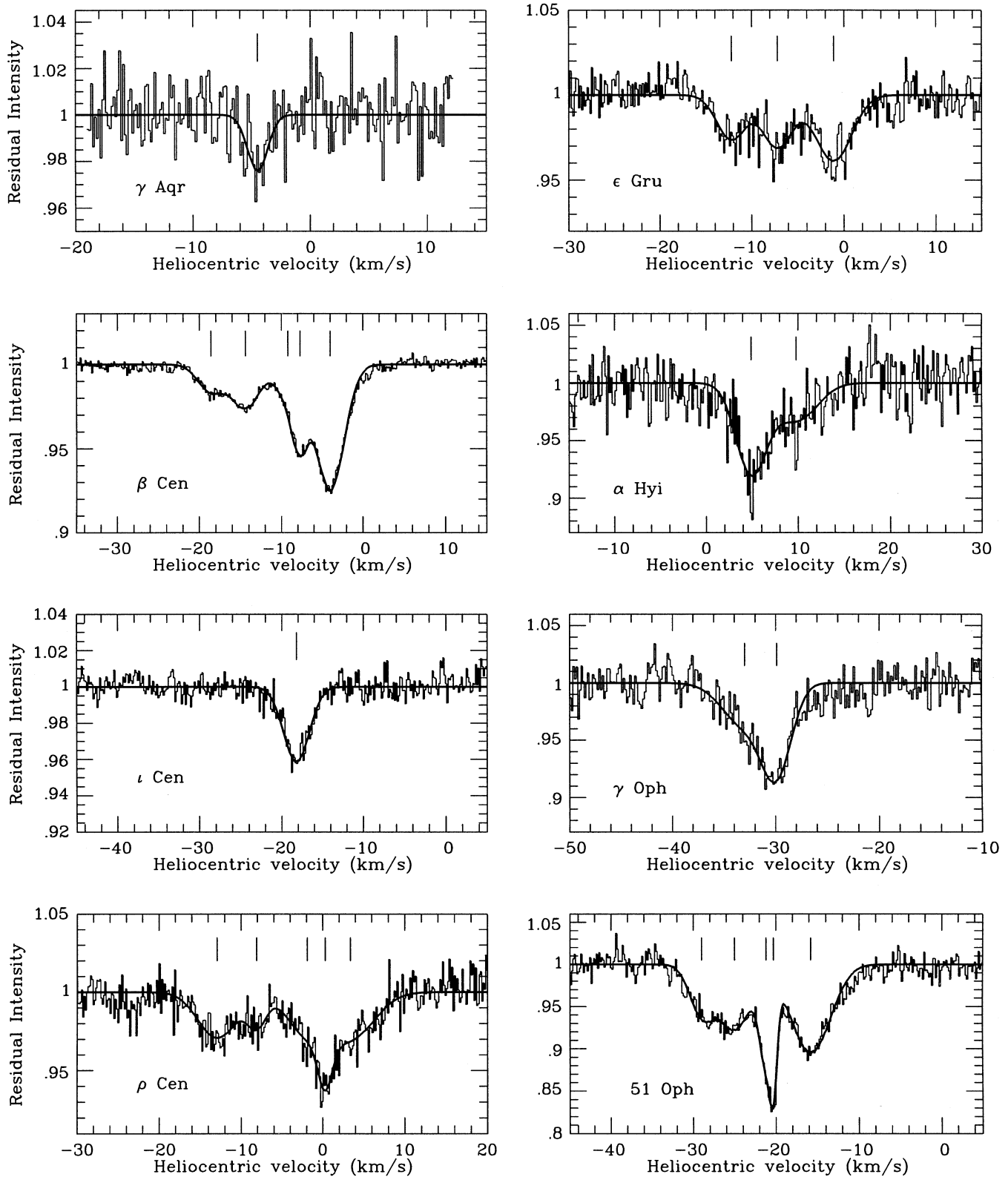


**Fig. 1.** The interstellar Ca K lines observed with the UHRF. The observed data are plotted as histograms. The smooth curves are theoretical line profiles with the parameters given in Table 2. The velocities of individual absorption components are indicated by vertical tick marks.

**Table 2.** Line profile parameters for the interstellar Ca K lines shown in Fig. 1, compared with other published values; a colon indicates that a previously published value is uncertain.  $W_\lambda$  is the total equivalent width (i.e. summed over all velocity components;  $2\sigma$  errors). Column 7 indicates whether a component falls within the velocity range occupied by the LIC or G clouds (Table 1; a question mark indicates that the component falls just outside the errors quoted on the cloud velocities), and also identifies possible circumstellar components (see text).

Star	$W_\lambda$ (here) (mÅ)	$W_\lambda$ (ref) (mÅ)	$v_{helio}$ (here) (km s <sup>-1</sup> )	$b$ (here) (km s <sup>-1</sup> )	$\log N$ (here) (cm <sup>-2</sup> )	Cloud ID	$v_{helio}$ (ref) (km s <sup>-1</sup> )	$b$ (ref) (km s <sup>-1</sup> )	Refs	
$\gamma$ Aqr	$0.6 \pm 0.2$	$0.4 \pm 0.2$	$-4.5 \pm 0.4$	$1.2^{+0.6}_{-0.4}$	$9.90^{+0.10}_{-0.20}$	LIC	$-4.4 \pm 0.7$	$2.9^{+1.2}_{-0.9}$	1	
$\beta$ Cen	$8.7 \pm 0.1$	8.1	$-18.6 \pm 0.1$	$2.2^{+0.2}_{-0.3}$	$9.98^{+0.06}_{-0.08}$	?G	-16.9	3:	2	
			$-14.4 \pm 0.1$	$2.4^{+0.2}_{-0.2}$	$10.23^{+0.05}_{-0.03}$	LIC	-13.8	1.5:		
			$-9.2 \pm 0.1$	$2.0^{+0.4}_{-0.4}$	$10.00^{+0.08}_{-0.30}$	}	-8.1	3:		
			$-7.7 \pm 0.1$	$1.4^{+0.2}_{-0.3}$	$10.16^{+0.14}_{-0.12}$					
			$-4.0 \pm 0.1$	$2.4^{+0.2}_{-0.2}$	$10.70^{+0.03}_{-0.04}$		-4.1	3:		
$\iota$ Cen	$2.2 \pm 0.2$	3:	$-18.2 \pm 0.1$	$2.2^{+0.2}_{-0.2}$	$10.40^{+0.05}_{-0.04}$	G	$-18.3 \pm 1.0$	3:	2,3	
$\rho$ Cen	$8.4 \pm 0.5$	$12 \pm 2$	$-12.9 \pm 0.2$	$3.3^{+0.3}_{-1.3}$	$10.42^{+0.05}_{-0.24}$	G	}	-12.5	$5.0^{+3.0}_{-2.0}$	4
			$-8.1 \pm 0.2$	$1.6^{+0.9}_{-0.6}$	$9.93^{+0.25}_{-0.23}$	?LIC				
			$-1.9 \pm 0.3$	$3.5^{+0.5}_{-1.5}$	$10.38^{+0.04}_{-0.20}$	}	-0.5	$4.0^{+3.0}_{-2.0}$		
			$+0.3 \pm 0.1$	$1.2^{+0.5}_{-0.4}$	$10.00^{+0.32}_{-0.15}$					
			$+3.4 \pm 0.2$	$4.1^{+0.9}_{-1.1}$	$10.51^{+0.09}_{-0.11}$					
$\epsilon$ Gru	$5.9 \pm 0.4$	$5.0 \pm 0.6$	$-12.2 \pm 0.2$	$2.2^{+0.5}_{-0.4}$	$10.20^{+0.08}_{-0.12}$	LIC	$-13.0 \pm 1.5$	2.9	3	
			$-7.2 \pm 0.1$	$2.3^{+0.5}_{-0.5}$	$10.29^{+0.12}_{-0.18}$		$-7.0 \pm 1.5$	2.6		
			$-1.1 \pm 0.1$	$2.7^{+0.3}_{-0.7}$	$10.46^{+0.08}_{-0.08}$		?C/S	$-1.1 \pm 1.5$		2.2
$\alpha$ Hyi	$7.1 \pm 0.7$	6.8	$+4.9 \pm 0.1$	$2.3^{+0.2}_{-0.8}$	$10.70^{+0.08}_{-0.16}$	G	+4.0:	2.0	3	
			$+9.8 \pm 0.4$	$3.2^{+0.8}_{-1.0}$	$10.46^{+0.14}_{-0.16}$		+8.0:	2.0		
$\gamma$ Oph	$6.1 \pm 0.4$	$7 \pm 2$	$-33.0 \pm 1.0$	$3.0^{+1.0}_{-1.0}$	$10.48^{+0.12}_{-0.30}$	}	-31.1 $\pm$ 1.0	3.3	3,5	
			$-29.9 \pm 0.3$	$2.0^{+0.5}_{-0.5}$	$10.62^{+0.16}_{-0.14}$					
51 Oph	$20.3 \pm 0.6$	$20 \pm 3$	$-29.0 \pm 0.2$	$2.0^{+0.5}_{-0.2}$	$10.52^{+0.13}_{-0.22}$	G	}	-26.9 $\pm$ 1.0	4.0	3,5
			$-25.0 \pm 0.3$	$2.8^{+0.7}_{-0.8}$	$10.78^{+0.12}_{-0.18}$	LIC				
			$-21.2 \pm 0.3$	$1.1^{+0.6}_{-0.3}$	$10.52^{+0.16}_{-0.42}$	?C/S	}	-21.3 $\pm$ 1.0	1.4	
			$-20.3 \pm 0.2$	$0.6^{+0.4}_{-0.1}$	$10.24^{+0.36}_{-0.05}$	?C/S				
			$-15.8 \pm 0.2$	$3.3^{+0.7}_{-0.3}$	$10.99^{+0.09}_{-0.04}$	C/S				

References: (1) Vallerga et al. (1993); (2) Lallement et al. (1986); (3) Bertin et al. (1993); (4) Crawford (1991); (5) Lagrange-Henri et al. (1990)

ponent by means of a Marquardt least-squares fitting program (described in more detail by Vallerga et al. 1993), and these are given in Table 2. The errors quoted on these values were obtained by an interactive estimation of the range of each parameter about the least-square value which is consistent with an acceptable overall fit. Although somewhat subjective, these error estimates are at least conservative (in most cases they are two to three times the formal  $1\sigma$  errors obtained by the least-square fitting program which, in order to reduce the computation time

to a manageable level, made the simplifying assumption that the errors on each component can be treated independently).

Table 2 also compares our results with those obtained by other authors at lower spectral resolution. It will be seen that, as expected, the new results mainly concern the discovery of velocity structure within components previously thought to be single, and the accurate measurement of velocity dispersions for components not properly resolved in earlier work. In this section we outline these new results, deferring a more detailed discussion of some of their implications to Sect. 4.

### 3.1. Equivalent widths

The equivalent widths were measured using the DIPSO spectral analysis program (Howarth, Murray & Mills 1993), and generally agree well with previously published values. This is reassuring because it indicates that the present observations have not been significantly affected by uncorrected scattered light, which would have caused our measurements to underestimate the actual values. This problem was noted in the earliest observations obtained with the UHRF, but it appears that the steps taken to correct it (discussed in Sect. 7.3 of Diego et al. 1995) have been successful.

### 3.2. Velocity structure

In Table 2 we use curly brackets to group together velocity components which we have resolved, but which lie within what appeared to be single components when observed at lower resolution. Six such cases were identified, towards four of the eight stars:

#### (i) $\beta$ Cen.

The  $-8.1 \text{ km s}^{-1}$  component observed by Lallement et al. (1986) with a resolution of  $3 \text{ km s}^{-1}$  is here resolved into two components, at  $-9.2$  and  $-7.7 \text{ km s}^{-1}$ .

#### (ii) $\rho$ Cen.

Earlier observations, obtained with a resolution of  $3.6 \text{ km s}^{-1}$  (Crawford 1991), identified two velocity components towards this star, whereas the present observations reveal five. The component previously identified at  $-12.5 \text{ km s}^{-1}$  is here split into two ( $-12.9$  and  $-8.1 \text{ km s}^{-1}$ ), which may plausibly be identified with the G and LIC clouds (see Sect. 4.1). In addition, the earlier  $-0.5 \text{ km s}^{-1}$  component is here resolved into three discrete components (at  $-1.9$ ,  $+0.3$ , and  $+3.4 \text{ km s}^{-1}$ ). Also, the unusually large  $b$ -value obtained for the  $+3.4 \text{ km s}^{-1}$  component ( $4.1^{+0.9}_{-1.1} \text{ km s}^{-1}$ ; Table 2) may indicate the presence of additional unresolved velocity structure.

#### (iii) $\gamma$ Oph.

The single component observed at  $-31.1 \text{ km s}^{-1}$  by Lagrange-Henri et al. (1990) is here resolved into components at  $-33.0$  and  $-29.9 \text{ km s}^{-1}$ . This structure will be discussed more fully in Sect. 4.2.

#### (iv) 51 Oph.

The Ca K line towards 51 Oph was observed at  $3 \text{ km s}^{-1}$  resolution by Lagrange-Henri et al. (1990), who identified three discrete velocity components (cf. their fig. 5). However, the higher-resolution observations presented here show that at least two of these are actually double, making a minimum of five components in all (Table 2). Lagrange-Henri et al.'s  $-26.9 \text{ km s}^{-1}$  component is resolved into two (at  $-29.0$  and  $-25.2 \text{ km s}^{-1}$ ), which correspond to the velocities expected for the G and LIC clouds (see Sect. 4.1). In addition, the narrow central component (at  $-21.3 \text{ km s}^{-1}$ ) is found to be double, and this will be discussed in Sect. 4.2.

### 3.3. Velocity dispersions

The velocity dispersions ( $b$ -values) found here are generally consistent with other published values (Table 2), when allowance is made for the lower resolution of earlier work and the previously unresolved blends discussed above. However, it is important to stress that the values measured here are much more accurately determined, owing to the order-of-magnitude higher resolution employed. As the observed line profiles are given by a convolution of the intrinsic profiles with the instrumental resolution, line profile modelling is insensitive to intrinsic velocity dispersions much smaller than the instrumental  $b$ -value ( $b_{inst}$ ). The previously published measurements referenced in Table 2 were all performed with  $b_{inst} \gtrsim 1.8 \text{ km s}^{-1}$  ( $R \lesssim 10^5$ ). This is comparable to the intrinsic widths of the lines being studied, and renders the resulting measurements somewhat uncertain. In contrast, the observations presented here were obtained with  $b_{inst} = 0.21 \text{ km s}^{-1}$ , with the result that all the velocity components have been fully resolved and therefore have well-determined velocity dispersions.

## 4. Discussion

In this section we elaborate on three specific aspects of these results: the nature of the LIC and G clouds; the nature and distribution of other nearby clouds; and the complicated interstellar and circumstellar spectrum of 51 Oph.

### 4.1. The LIC and G clouds

As discussed in Sect. 1, one of the unsolved questions concerning the structure of the local interstellar medium is the relationship between the Local Interstellar Cloud itself, and the G cloud identified by Lallement & Bertin (1992). As discussed by Lallement et al. (1995; their Sect. 1.3), the main difficulty is the small projected velocity difference between the LIC and G cloud velocity vectors. As this is always less than  $3 \text{ km s}^{-1}$  (Sect. 1), lower-resolution studies have found it difficult to determine whether *both* clouds are present towards any given star. Detection of both components would argue strongly for the LIC and G clouds being separate entities, while detection of only one or the other would argue for a velocity gradient within a single cloud.

With this in mind, Table 1 lists the velocities of the LIC and G clouds, projected towards the stars observed here, and Table 2 identifies those components which fall within the uncertainties on the projected cloud velocities. It will be seen that components at the LIC and/or G cloud velocities are detected towards seven of the eight stars (the exception being  $\gamma$  Oph, which is discussed further in Sect. 4.2), but only in one case (51 Oph) are absorption components found which lie within the velocity ranges expected for *both* clouds. Since a single exception could be explained away as a coincidence, this lack of dual detections would seem to argue against the LIC and G clouds being separate entities. However, the situation is complicated by the fact that: (1) two stars ( $\beta$  Cen and  $\rho$  Cen) only fail to exhibit both components because in each case one lies outside the

predicted range by  $\lesssim 0.5 \text{ km s}^{-1}$  (these components are identified by question marks in Table 2); and (2) Crawford & Dunkin (1995) plausibly identified both components in the line of sight to  $\alpha$  Oph ( $l = 35.9^\circ$ ,  $b = +22.6^\circ$ ,  $D = 15 \text{ pc}$ ).

In spite of these uncertainties, some trends are suggested by the present data. In particular, there is a tendency for the LIC to be observed either on its own or not at all at high negative latitudes ( $-60^\circ \lesssim b \lesssim -40^\circ$ : i.e. towards  $\gamma$  Aqr,  $\epsilon$  Gru,  $\alpha$  Gru; cf. Crawford & Dunkin 1995 for the latter star), whereas the stars which may plausibly be interpreted as exhibiting components due to both clouds ( $\beta$  Cen,  $\rho$  Cen, 51 Oph,  $\alpha$  Oph) lie at low positive latitudes ( $0^\circ \lesssim b \lesssim +25^\circ$ ). However, the fact that a component at the G cloud velocity is detected without the LIC towards stars as well-separated in latitude as  $\iota$  Cen ( $b = +25.8$ ) and  $\alpha$  Hyi ( $b = -53.8$ ), and that neither cloud was detected towards  $\gamma$  Oph or  $\alpha$  Eri (Crawford & Dunkin 1995), means that a simple picture in which lines of sight towards stars at low positive latitudes pass through both the LIC and the G clouds is probably untenable (unless both clouds are very inhomogeneous). Only by obtaining many more observations of nearby stars, performed with sufficient spectral resolution to discriminate between the LIC and G cloud velocities, will it be possible to shed further light on the spatial extent of these two clouds, and we hope to obtain such observations in the near future.

Regardless of the spatial distribution of the LIC and G Cloud velocity components, the present observations are able to provide new information on the physical conditions prevailing within this material. For Ca ions, the velocity dispersion is related to the kinetic temperature,  $T_k$ , and the line-of-sight rms turbulent velocity,  $v_t$ , by

$$b = \sqrt{0.413 \left( \frac{T_k}{1000\text{K}} \right) + 2v_t^2} \quad \text{kms}^{-1}. \quad (1)$$

The five components identified with the LIC in Table 2 have well-defined  $b$ -values in the range  $1.2$  to  $2.4 \text{ km s}^{-1}$ . Allowing for the errors, all but one of these values is consistent with other indications of the physical conditions prevailing in the LIC (cf. Sect. 1). Specifically, Equation 1 gives  $b = 2.2 \text{ km s}^{-1}$  for  $T_k = 7000 \text{ K}$  and  $v_t = 1.0 \text{ km s}^{-1}$ , and this falls within the errors on the observed  $b$ -values for every LIC component except that towards  $\gamma$  Aqr. We may also note that these values of temperature and turbulence are consistent with the  $b$ -values obtained for velocity components identified with the G cloud, underscoring the fact that, if the two clouds are physically separate, they nevertheless have similar internal physical conditions.

The single absorption component observed towards  $\gamma$  Aqr is exceptional because, while the velocity is essentially identical to that expected for the LIC, its  $b$ -value ( $1.2_{-0.4}^{+0.6} \text{ km s}^{-1}$ ) implies an upper limit to the temperature ( $3500_{-1900}^{+4400} \text{ K}$ ) which is lower than that obtained for other LIC sightlines. It is true that temperatures at the upper end of this range are consistent with the canonical LIC value of  $7000 \text{ K}$ , but Equation 1 shows that such a temperature is only possible if  $v_t \lesssim 0.4 \text{ km s}^{-1}$ . Thus it seems that the region of the LIC present towards  $\gamma$  Aqr is cooler and/or less turbulent than elsewhere. Observations of additional

stars, close to  $\gamma$  Aqr on the sky, will be required to determine the physical extent of this cooler/less turbulent region.

#### 4.2. Other nearby clouds

The present observations reveal the presence of 14 velocity components (towards six of the eight stars) in addition to the ten already tentatively identified with the LIC and G clouds (Table 2). Excluding the three towards 51 Oph, which are probably circumstellar in origin (and which are discussed in Sect. 4.3), and one possibly circumstellar component towards  $\epsilon$  Gru (Bertin et al. 1993), this leaves ten components which arise in additional low density clouds within the Local Bubble. As discussed in Sect. 3.2, many of these components have here been resolved for the first time, and, as might be expected, the two most distant stars ( $\beta$  Cen and  $\rho$  Cen, both at about  $80 \text{ pc}$ ) exhibit the largest number of components (cf. Table 2).

Most of these components have velocity dispersions which suggest physical conditions similar to those deduced for the LIC and G clouds. Specifically, all but three have  $b$ -values that are consistent with  $T_k \sim 7000 \text{ K}$  and  $v_t \approx 1 \text{ km s}^{-1}$  (i.e.  $b \approx 2.2 \text{ km s}^{-1}$ , allowing for the errors). The  $+3.4 \text{ km s}^{-1}$  component towards  $\rho$  Cen ( $b = 4.1_{-1.1}^{+0.9} \text{ km s}^{-1}$ ) is broader than might be expected, but, as noted in Sect. 3.2, this probably results from the presence of an additional unresolved velocity component. Of greater interest are the two components (i.e. those at  $-7.7 \text{ km s}^{-1}$  towards  $\beta$  Cen, and  $+0.3 \text{ km s}^{-1}$  towards  $\rho$  Cen) which have  $b$ -values ( $1.4_{-0.3}^{+0.2}$  and  $1.2_{-0.4}^{+0.5} \text{ km s}^{-1}$ , respectively) which are lower than expected, and similar to that of the anomalously narrow LIC component identified towards  $\gamma$  Aqr. Indeed, these two clouds must be rather cooler and/or less turbulent than that towards  $\gamma$  Aqr as the  $b$ -value upper limits are lower – implying rigorous temperature upper limits of  $T_k \sim 6200 \text{ K}$  for  $\beta$  Cen, and  $T_k \sim 7000 \text{ K}$  for  $\rho$  Cen. Conversely, by assuming  $T_k = 0$ , we obtain rigorous upper limits to  $v_t$  of  $1.1$  and  $1.2 \text{ km s}^{-1}$  for these components. Since, in reality, there will be some trade-off between  $T_k$  and  $v_t$ , the actual values of both must lie below these limits.

The line of sight towards  $\gamma$  Oph deserves special comment, because of what it tells us about the complicated state of the LISM in the direction of Ophiuchus. As noted in Sect. 4.1,  $\gamma$  Oph is the only star in the present sample which does not exhibit clear evidence for an absorption component at either of the LIC or G cloud velocities. This is all the more remarkable when one considers that  $\gamma$  Oph is bracketed on the sky by  $\alpha$  Oph and 51 Oph (with angular separations of  $10.4^\circ$  and  $27.0^\circ$ , respectively), and that both of these neighbouring stars do have components at the G and LIC velocities (for  $\alpha$  Oph, see Crawford & Dunkin 1995). It is true that the spectrum of  $\gamma$  Oph shown in Fig. 1 does reveal some evidence for very weak ( $\lesssim 1$ - $2\%$  deep) absorption in the velocity range occupied by the LIC and G clouds (i.e.  $-26.7$  to  $-24.2 \text{ km s}^{-1}$ ; cf. Table 1), but, given the signal-to-noise ratio of the data, this is barely significant. Formally, the column density upper limits for components assumed to be present at the LIC and G cloud velocities are  $\log N \lesssim 9.90$  (assuming  $b = 2.2 \text{ km s}^{-1}$ ; the upper limits are lower for narrower lines). This is

comparable to the LIC column density deduced for  $\gamma$  Aqr, but is approximately an order of magnitude lower than those found for  $\alpha$  Oph and 51 Oph. Thus, while the present non-detection is still consistent with the LIC being present towards  $\gamma$  Oph (as it would have to be if it truly surrounds the Sun), the upper limit implies order-of-magnitude spatial and/or density inhomogeneities on a scale of  $\lesssim 0.2$  pc (based on the angular separation of  $\gamma$  Oph and  $\alpha$  Oph, and an assumed LIC extent of  $\lesssim 1$  pc in this direction; cf. Lallement et al. 1994).

The two stronger, more blue-shifted, components which are observed towards  $\gamma$  Oph must be due to other, probably more distant, clouds. Indeed, components with similar velocities ( $-32.0$  and  $-28.4$  km s $^{-1}$ ), and similar column densities and  $b$ -values, were observed towards  $\alpha$  Oph by Crawford & Dunkin (1995), so it appears likely that the same two clouds have also been sampled by this line of sight. At the distance of the nearer of the two stars ( $\alpha$  Oph,  $D = 15$  pc) the lines of sight are separated by 2.7 pc, which is consistent with other estimates of the sizes of clouds within the local bubble. However, we note that Barlow et al. (1995) detected a weak ( $\log N = 10.20$  cm $^{-2}$ ) Ca II component at  $-31.8$  km s $^{-1}$  towards  $\zeta$  Oph ( $l = 6.3^\circ$ ,  $b = +23.6^\circ$ ,  $D = 230$  pc), which may imply that this line of sight has also passed through the material responsible for the most negative velocity component present towards  $\gamma$  Oph. As the separation of these two lines of sight at the distance of  $\alpha$  Oph is 6 pc, and as this is rather larger than previous estimates for the sizes of the local clouds, this cloud may actually be quite a lot closer than  $\alpha$  Oph.

The strongest absorption component towards  $\alpha$  Oph (i.e. that at  $-26.2$  km s $^{-1}$ ) is not observed towards  $\gamma$  Oph, and this is consistent with the view of Frisch, York & Fowler (1987) that  $\alpha$  Oph lies behind a ‘wisp’ of H I emission which they identified in the 21-cm maps of Colomb, Pöppel & Heiles (1980). However, it will be necessary to observe the interstellar spectra of many more nearby stars in Ophiuchus, and these at a range of distances, before we can be certain that the 21-cm structures observed in this direction by Colomb et al. are really as close (i.e. within 15 pc of the Sun) as this argument would imply.

#### 4.3. The spectrum of 51 Oph

The spectrum of 51 Oph is interesting for a variety of reasons. In addition to the two components tentatively identified with the LIC and G clouds (Sect. 4.1), three other absorption components are present towards this star. Perhaps of greatest interest is the fact that the narrow central ( $-21.3$  km s $^{-1}$ ) component identified by Lagrange-Henri et al. (1990) is asymmetric, which implies the presence of additional velocity structure. Fig. 2a shows this component plotted on an expanded scale, which emphasises the asymmetry of the profile, and also shows our two-component fit (Table 2). Both of these components are extremely narrow, and the velocity dispersion of the  $-20.3$  km s $^{-1}$  component ( $b = 0.6^{+0.4}_{-0.1}$  km s $^{-1}$ ) implies an upper limit to the kinetic temperature (obtained by assuming  $v_t = 0$  in Equation 1) of  $870^{+1550}_{-270}$  K, which is much lower than that expected for clouds within the Local Bubble (Sect. 1). It is true that several

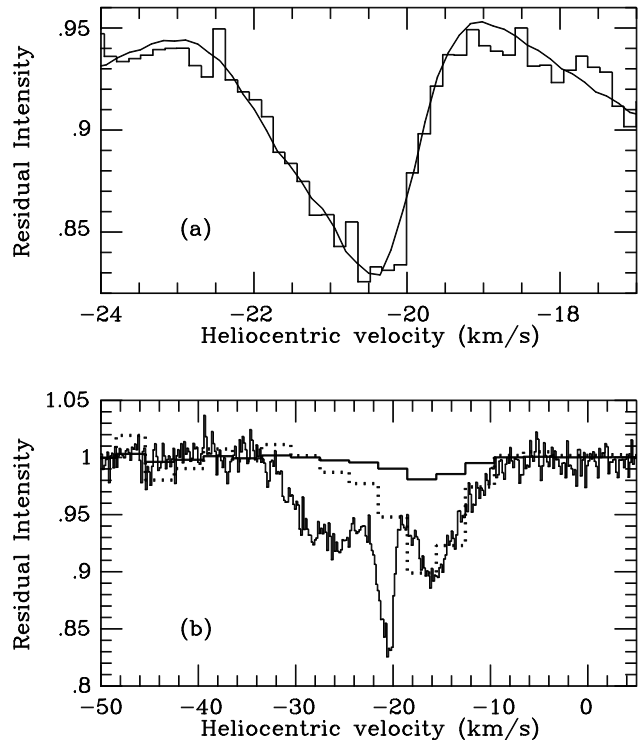


**Fig. 2.** **a** An expanded view of the central narrow ( $-21.3$  km s $^{-1}$ ) component towards 51 Oph, showing the asymmetry of the line profile. The theoretical two-component model profile (Table 2) is also shown. **b** Comparison of the UHRF Ca K spectrum of 51 Oph with a lower resolution observation of the line due to excited Fe II (Dunkin et al. 1996). The solid line shows the normalised Fe II spectrum, while the dotted line shows the same line scaled to the depth of the  $-15.8$  km s $^{-1}$  Ca II component. Clearly the Fe II is mostly associated with this particular Ca II component; see text for discussion.

comparably narrow Ca II components were detected in UHRF observations of  $\zeta$  Oph by Barlow et al. (1995), but these were found to be associated with the complex of components centered at about  $-14$  km s $^{-1}$ , and which are known to be associated with more distant cold molecular clouds. Thus, either the line-of-sight to 51 Oph has passed through an unusually cool cloud within 25pc of the Sun (which is not observed towards other nearby stars in Ophiuchus), or these narrow components arise in the circumstellar environment.

As 51 Oph is a well known Vega-excess star (i.e. a main-sequence star exhibiting an infrared excess due to circumstellar dust; Coté & Waters 1987, Waters, Coté & Geballe 1988), it is quite likely that some of the absorption components have a circumstellar origin (Lagrange-Henri et al. 1990). Indeed, quite convincing evidence that at least the  $-15.8$  km s $^{-1}$  component, and possibly the narrow central components also, are circumstellar comes from the detection of the 4583.837 Å line of Fe II by Dunkin, Barlow & Ryan (1996). This line is not observed in the general interstellar medium because it arises from a metastable level ( $3d^64s(^4F_{9/2})$ ) which lies 2.8 eV above the ground state. The fact that this level is populated strongly



suggests excitation in the circumstellar environment, a point already made by Grady & Silvis (1993) in connection with their detection of UV lines from excited levels of Fe II towards this star. Fig. 2b shows the Fe II line observed at  $R = 44000$  (S.K. Dunkin, personal communication) superimposed on the UHRF spectrum of the Ca K line. Even allowing for the lower resolution of the Fe II spectrum, it is clear that this line is centered at the velocity of the  $-15.8 \text{ km s}^{-1}$  Ca II component (this is especially obvious if the Fe II line is scaled to the same depth as the Ca II component; dotted line in Fig. 2b). Inspection of Fig. 2b also shows that the Fe II line is asymmetric, indicative of additional Fe II absorption blueward of  $-15.8 \text{ km s}^{-1}$ . This is the velocity range occupied by the narrow central components, and may suggest that these are also circumstellar. Only UHRF observations of the Fe II line itself will be able to determine unambiguously whether or not this is the case.

Given these arguments for a circumstellar origin, it is of particular interest to determine whether or not these lines exhibit line-profile variations similar to those found for the well-studied  $\beta$  Pictoris system (e.g. Ferlet, Hobbs & Vidal-Madjar 1987, Lagrange-Henri et al. 1992, Crawford et al. 1994). This is especially important as Grady & Silvis (1993) have found clear evidence for in-falling gas (with velocities up to  $100 \text{ km s}^{-1}$ ) from time-variable, redshifted UV absorption lines in 51 Oph which are very similar to those found for  $\beta$  Pic. In order to check for such variations in the Ca K line, we degraded our UHRF spectrum to an effective resolution of  $R = 10^5$ , and compared it with that obtained by Lagrange-Henri et al. (1990). This comparison revealed no evidence for spectral changes, either in the velocities or in the relative intensities of the absorption components. Thus, while further ultra-high-resolution monitoring of the line profile will be needed before a definite conclusion can be reached, the present observations show no evidence for  $\beta$  Pic-type variability in the circumstellar Ca II line of 51 Oph.

As a final point, we note that the constancy in velocity of the (presumed) circumstellar line profiles (Table 2) is doubly surprising given that Buscombe (1963) found 51 Oph to have a variable velocity. If this star really is a spectroscopic binary, and if, as seems almost certain, the  $-15.8 \text{ km s}^{-1}$  component arises in the circumstellar environment, it would appear that the circumstellar material must surround both stars. On the other hand, it may be that the assignment of a variable stellar velocity is spurious. Clearly it would be desirable to obtain more accurate measurements of the stellar radial velocity in order to settle this question.

## 5. Conclusions

We have used the Ultra-High-Resolution Facility (UHRF) at the Anglo-Australian Telescope to study interstellar Ca K lines towards eight nearby stars. The spectral resolution ( $0.35 \text{ km s}^{-1}$ , FWHM) was sufficient for us to fully resolve the intrinsic line profiles. This has enabled us to detect hitherto unresolved velocity structure in the LISM, and to obtain accurate measurements of the velocity dispersions ( $b$ -values) of the local clouds. Our principal conclusions are as follows:

(1) Absorption components at the velocities expected for the LIC and/or the G cloud (Lallement et al. 1995) have been detected towards all but one star ( $\gamma$  Oph). The column density upper limits deduced for  $\gamma$  Oph ( $\log N(\text{Ca II}) \lesssim 9.90 \text{ cm}^{-2}$ ) are consistent with the LIC and/or G cloud being present towards this star, but only by assuming order-of-magnitude spatial and/or density inhomogeneities on sub-parsec scales. Only in the case of one star (51 Oph) is there a fairly secure detection of *both* the LIC and G clouds.

(2) The velocity dispersions deduced for the LIC/G cloud components are generally consistent with other determinations of the physical conditions prevailing in the LIC ( $T_k \approx 7000 \text{ K}$ ,  $v_t \approx 1 \text{ km s}^{-1}$ ). However, the weak LIC component towards  $\gamma$  Aqr is narrower than expected ( $b = 1.2_{-0.4}^{+0.6}$ ), suggesting that the LIC in this direction is cooler and/or less turbulent than elsewhere. Observations of other nearby stars, close to  $\gamma$  Aqr on the sky, are needed to determine the extent of this apparently anomalous region.

(3) The velocity dispersions of the other (i.e. non-LIC/G cloud) velocity components suggest temperature/turbulence regimes similar to that of the LIC. However, the two most distant stars in the present sample ( $\beta$  Cen and  $\rho$  Cen) also exhibit narrower components which must arise in a somewhat cooler and/or less turbulent environment.

(4) Five absorption components were identified towards the nearby Vega-excess star 51 Oph. Two were identified with the LIC and G clouds (Table 2). Of the others, that at  $-15.8 \text{ km s}^{-1}$  is almost certainly circumstellar, owing to its association with an excited metastable state of Fe II (Fig. 2b; Dunkin et al. 1996). The two remaining components (at  $-21.2$  and  $-20.3 \text{ km s}^{-1}$ , which are here resolved for the first time; cf. Fig. 2a) are very narrow by LISM standards, and may also arise in the circumstellar environment (Sect. 4.3). However, allowing for the differences in spectral resolution, we found no evidence for any change in the Ca K line profile between the observations reported here and those obtained by Lagrange-Henri et al. (1990).

*Acknowledgements.* We are thank S.K. Dunkin for providing the Fe II spectrum of 51 Oph, and PATT for the award of telescope time. IAC is grateful to PPARC for the award of a post-doctoral research fellowship and to M.J. Barlow for support and encouragement.

## References

- Barlow, M.J., Crawford, I.A., Diego, F., Dryburgh, M., Fish, A.C., Howarth, I.D., Spyromilio, J., Walker, D.D., 1995, MNRAS, 272, 333
- Bertaux, J.L., Lallement, R., Kurt, V.G., Mironova, E.N., 1985, A&A, 150, 1
- Bertin, P., Lallement, R., Ferlet, R., Vidal-Madjar, A., 1993, A&A, 278, 549
- Breitschwerdt, D., Schmutzler, T., 1994, Nature, 371, 774
- Buscombe, W., 1963, MNRAS, 126, 29
- Chassefière, E., Dalaudier, F., Bertaux, J.L., 1988, A&A, 201, 113
- Colomb, F.R., Pöppel, W.G.L., Heiles, C., 1980, A&AS, 40, 47
- Coté, J., Waters, L.B.F.M., 1987, A&A, 176, 93

- Cox, D.P., Reynolds, R.J., 1987, *ARA&A*, 25, 303
- Crawford, I.A., 1991, *A&A*, 247, 183
- Crawford, I.A., Dunkin, S.K., 1995, *MNRAS*, 273, 219
- Crawford, I.A., Spyromilio, J., Barlow, M.J., Diego, F., Lagrange, A.M., 1994, *MNRAS*, 266, L65
- de Geus, E.J., de Zeeuw, P.T., Lub, J., 1989, *A&A*, 216, 44
- Diamond, C.J., Jewell, S.J., Ponman, T.J., 1995, *MNRAS*, 274, 589, 1995
- Diego, F., 1993, *Appl. Opt.*, 32, 6284
- Diego, F., et al., 1995, *MNRAS*, 272, 323
- Dunkin, S.K., Barlow, M.J., Ryan, S.G., *MNRAS*, in preparation
- Ferlet, R., Hobbs, L.M., Vidal-Madjar, A., 1987, *A&A*, 185, 267
- Frisch, P.C., 1995, *Space Sci. Rev.*, 72, 499
- Frisch, P.C., York, D.G., Fowler, J.R., 1987, *ApJ*, 320, 842
- Grady, C.A., Silvis, J.M.S., 1993, *ApJ*, 402, L61
- Howarth, I.D., Murray, J., Mills, D., 1993, *Starlink User Note*, No. 50
- Jelinsky, P., Vallerga, J.V., Edelstein, J., 1995, *ApJ*, 442, 653
- Lagrange-Henri, A.M., Ferlet, R., Vidal-Madjar, A., Beust, H., Gry, C., Lallement, R., 1990, *A&AS*, 85, 1089
- Lagrange-Henri, A.M., Gosset, E., Beust, H., Ferlet, R., Vidal-Madjar, A., 1992, *A&A*, 264, 637
- Lallement, R., Bertin, P., 1992, *A&A*, 266, 479
- Lallement, R., Vidal-Madjar, A., Ferlet, R., 1986, *A&A*, 168, 225
- Lallement, R., Bertin, P., Ferlet, R., Vidal-Madjar, A., Bertaux, J.L., 1994, *A&A*, 286, 898
- Lallement, R., Ferlet, R., Lagrange, A.M., Lemoine, M., Vidal-Madjar, A., 1995, *A&A*, 304, 461
- Lesh, J.R., 1972, *A&AS*, 5, 129
- Linsky, J.L., et al., 1993, *ApJ*, 402, 694
- Linsky, J.L., Diplas, A., Wood, B.E., Brown, A., Ayres, T.R., Savage, B.D., 1995, *ApJ*, 451, 335
- Linsky, J.L., Wood, B.E., 1996, *ApJ*, in press
- McCammon, D., Burrows, D.N., Sanders, W.T., Kraushaar, W.L., 1983, *ApJ*, 269, 107
- McCammon, D., Sanders, W.T., 1990, *ARA&A*, 28, 657
- Shortridge, K., 1988, *Starlink User Note*, No. 86
- Vallerga, J.V., Vedder, P.W., Craig, N., Welsh, B.Y., 1993, *ApJ*, 411, 729
- van Altena, W.F., Lee, J., Hoffleit, D., 1991, *New Yale General Catalogue of Trigonometric Stellar Parallaxes*, Yale University Observatory, New Haven
- Vennes, S., et al., 1994, *ApJ*, 421, L35
- Waters, L.B.F.M., Coté, J., Geballe, T.R., 1988, *A&A*, 203, 348
- Welsh, B.Y., Craig, N., Vedder, P.W., Vallerga, J.V., 1994, *ApJ*, 437, 638
- Witte, M., Rosenbauer, H., Banaszekiewicz, M., Fahr, H., 1993, *Adv. Space Res.*, 13, (6), 121